

TURBULENCE AND ELECTRON HEATING IN TWO-STREAM INSTABILITY

V. T. ASTRELIN, N. S. BUCHELNIKOVA, A. A. DROZDOV, and A. M. KUDRYAVTSEV

Nuclear Physics Institute, Siberian Division, USSR Academy of Sciences

Submitted October 22, 1969

Zh. Eksp. Teor. Fiz. 58, 1553–1566 (May, 1970)

High-frequency plasma wave instability excited by an electron beam in a plasma of restricted radius is investigated experimentally. The space-time correlation functions of the high-frequency oscillations are measured and the $\varphi_{k\omega}^2$ spectra for various operating conditions are determined on their basis. Nonresonant plasma electron heating is observed and its relation to the $\varphi_{k\omega}^2$ oscillation spectrum is investigated. The heating mechanism is shown to be stochastic.

THE interaction of beams of charged particles with plasma has been the subject of an appreciable number of theoretical and experimental studies^[1], in which a wide class of instabilities excited in such interactions were observed and investigated. In many experiments, considerable plasma heating was observed upon development of two-stream instability^[2-5]. Plasma turbulence was investigated in a number of studies^[6-8].

We have investigated the interaction between an electron beam and a strongly ionized potassium plasma produced independently of the beam. We investigated the beam-excited HF instability on plasma Langmuir waves, the turbulent state of the plasma, and the mechanism of electron heating by the fields of HF oscillations.

DESCRIPTION OF SETUP AND MEASUREMENT PROCEDURES

1. The experiments were performed with the setup illustrated in Fig. 1. A vacuum chamber of 15 cm diameter and 144 cm length was evacuated to $\sim 5 \times 10^{-6}$ Torr. The stationary magnetic field strength was 500–1000 Oe. The field inhomogeneity along the axis did not exceed 1%, and the length of the homogeneous-field region was 100 cm. The plasma was produced by thermal ionization of potassium vapor on a tungsten plate (ionizer) of 4 cm diameter, heated to $T \sim 2300^\circ\text{K}$. The plasma column was bounded in length by a disc with an aperture, and a potential on the order of the floating potential of the plasma was applied to the disc; the column was 80 cm. The plasma density was maximal on the axis and decreased along the radius. The experiments were performed at a plasma density on the axis $n_0 \sim (0.1-10) \times 10^9 \text{ cm}^{-3}$.

The electron beam was produced by an electron gun located in the region of homogeneous magnetic fields. The energy of the beam electrons was $U_0 \sim 20-600 \text{ eV}$, the current $I_0 \sim 0.3-20 \text{ mA}$, and the beam diameter 1 cm.

2. The plasma density was determined from the saturation electron current of a planar probe oriented across the magnetic field and located outside the beam^[9].

The HF oscillations of the potential were registered with HF probes. The probe was constructed in the form of a coaxial cable matched to the measuring systems, having a SWR not worse than 1.4 in the 20–1000 MHz

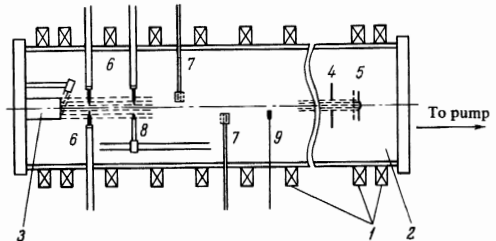


FIG. 1. Experimental setup: 1—magnetic field coil, 2—vacuum volume, 3—ionizer, 4—limiting disc, 5—electron gun, 6—high-frequency probes, 7—longitudinal-energy analyzers, 8—movable high-frequency probe, 9—flat probe.

range. The working part of the probe was a segment of the central conductor projecting from the coaxial cable, with diameter $d = 0.025 \text{ cm}$ and length $l = 0.2 \text{ cm}$. The working part of the probe used for the measurement of the absolute values of the amplitude of the potential was covered with glass and had $d = 0.05 \text{ cm}$ and $l = 0.3 \text{ cm}$. Since the surface of the glass was charged in the plasma to a large negative potential, on the order of the floating potential, a layer of radius r_l was produced around the probe, and in this layer there were practically no electrons, $n_e \ll n_0$. If the oscillations are electrostatic, then the probe-plasma system is equivalent to a cylindrical capacitor, where the role of the inner electrode is played by the segment of the central conductor, and the role of the outer electrode by the plasma “moved away” from the probe to a distance $\sim r_l$. If the wavelength of the potential oscillations λ is much larger than r_l , the entire internal electrode has the same potential $\varphi(t)$ relative to the internal electrode, which is grounded through a small resistance R_{meas} . As a result, the measured potential is related to the potential in the plasma:

$$\varphi_{\text{meas}} = iR_{\text{meas}} = \varphi R_{\text{meas}} / \sqrt{R_{\text{meas}}^2 + (\omega C_{\text{pr-p}})^{-2}}$$

Here $C_{\text{pr-p}}$ is the probe-plasma capacitance (the capacitance of the glass screen can be disregarded, since it is much larger than $C_{\text{pr-r}}$). The value of $C_{\text{pr-p}}$ is determined by the dimension of the layer r_l , which can be determined by using the results of^[9]. It turned out that under the experimental conditions at $T_e \gtrsim 2 \text{ eV}$ and $n_0 \lesssim 10^9 \text{ cm}^{-3}$ we have $r_l \gtrsim l$ (but $r_l \ll \lambda$). This circumstance allows us to regard under these conditions the

probe-plasma capacitance to be approximately equal to the capacitance of a solitary post:

$$C_{pr-p} = C_s = \sqrt{l^2 - d^2} / 2 \ln \frac{l + \sqrt{l^2 - d^2}}{d}.$$

We note that allowance for the outer electrode at $r_l = l$ increases the value of C_{pr} by only 20%. Thus, at $T_e > 2$ eV and $n_0 \lesssim 10^9$ cm⁻³, the probe-plasma capacitance does not depend on the parameters of the plasma and on the oscillations, and is determined only by the geometry of the probe. Since in our case $C_{pr} = 0.07$ pF and $1/\omega C_{pr} \gg R_{meas}$ in the working frequency region, the connection between φ_{meas} and φ becomes quite simple:

$$\varphi_{meas} = R_{meas} \omega C_s \varphi.$$

In the measurements of the frequency spectra of the oscillations we used receivers of the type P5-1–P5-3, which cover the frequency band 20–1800 MHz, with sensitivity ~ 5 μ V. We also use panoramic spectrum analyzers^[10] with a frequency range 30–1000 MHz and sensitivity ~ 200 μ V. We note that we measured with the aid of the receivers and the spectrum analyzers the effective amplitude of the oscillations $\bar{\varphi} = (\varphi^2)^{1/2}$ in a bandwidth $\Delta f \sim 0.1$ –1 MHz, depending on the type of the receiver. The quantity $\bar{\varphi}^2$, which characterizes the total power of the oscillation, was measured with the aid of a broadband detector head.

3. The correlation measurements were made with the aid of a microwave correlation meter (Fig. 2) with a frequency range 20–20,000 MHz and a sensitivity ~ 1 mV^[11]. The non-uniformity of the amplitude-frequency characteristic of the correlation meter did not exceed 3 dB. The signal delay τ was effected with the aid of a delay line constructed of segments of coaxial cable. The value of τ could be changed from zero to 100 nsec in steps of 0.1 nsec.

The correlation meter made it possible to determine the normalized space-time correlation function (STCF) of the oscillations of the potential $\varphi(\mathbf{r}, t)$:

$$\rho(\xi, \tau) = \overline{\varphi(\mathbf{r}, t)\varphi(\mathbf{r} + \xi, t + \tau)} / \{\overline{\varphi^2(\mathbf{r}, t)\varphi^2(\mathbf{r} + \xi, t)}\}^{1/2},$$

where ξ is the distance between probes. The STCF is the auto-correlation function (ACF) of the oscillations at $\xi = 0$, the spatial correlation function (SCF) at $\tau = 0$, and the mutual correlation function (MCF) at $\xi = \text{const}$.

Measurements of the CF were performed in the half of the plasma column closest to the ionizer, at a length $\Delta z \sim 20$ cm. From the CF we determined the following characteristics of the potential oscillations in the plasma:

a) The mean values of the frequency of the spectrum and of the wave vector—from the period of the CF; the

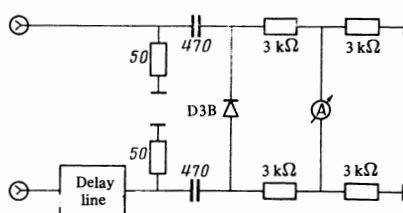


FIG. 2. Diagram of the correlation meter.

time and length of the correlation—from the attenuation of the envelope by a factor of e.

b) The direction of propagation and the average phase velocity of the oscillations \bar{v}_{ph} —from the displacements between the maxima of the MCF, measured in different points at a distance ξ : $\bar{v}_{ph} = \xi/\Delta\tau$.

c) The power spectra $\varphi_{k_z\omega}^2$, φ_ω^2 , and $\varphi_{k_z}^2$ —by applying the Fourier transformation to the corresponding CF:

$$\varphi_{k_z\omega}^2 = \frac{1}{(2\pi)^2} \overline{\varphi^2} \iint \rho(\Delta z, \tau) \cos k_z \Delta z \cos \omega \tau d(\Delta z) d\tau.$$

Here $\overline{\varphi^2}$ is the mean squared amplitude of the potential oscillations.

To check on the correctness of the correlation measurements and their recalculation, we compared the calculated spectrum $\varphi_\omega^2 = \int \varphi_{k_z\omega}^2 d k_z$ with the frequency spectrum measured by the panoramic analyzer. The following should be noted in this case. The calculated spectrum φ_ω^2 is determined by the dependence of $\rho(\Delta z, \tau)$ on τ . Since in the experiment $\rho(\Delta z, \tau)$ is measured as a set of SCF $\rho_z(\Delta z)$ at different values of τ , this dependence is determined by the entire set of SCF, and not by direct measurement. Therefore the calculated spectrum $\varphi_{k_z\omega}^2$ contains all the errors of both the measurements and of the recalculation. A comparison of the spectrum has shown that they practically coincide.

4. The plasma and beam electron energy distributions were investigated with the aid of two-grid electrostatic analyzers. The analyzing potential V was applied on the grid located near the collector, and the collector itself was under positive potential. The external grid was grounded. Special measurements have shown that such “parasitic” effects as the influence of the secondary electrons knocked out from the electrodes of the analyzer by the fast particles, the overhang of the plasma into the region of the analyzing grid, and the formation of space charge by the current of the analyzing electrons did not influence the measurements in our case. The distribution function was determined from the current-voltage characteristic I(V) of the collector. We note that for a Maxwellian distribution $\ln I(V)$ has the form of a straight line, the slope of which determines the longitudinal electron temperature T_e . For a qualitative description of the plasma electrons, we introduced a “limiting” energy ϵ , determined from the condition $I(\epsilon) = 0.1 I(0)$.

5. The experiments were performed in the electron-layer regime, and in the absence of the beam the plasma was “quiescent”—there were practically no oscillations, and the diffusion across the magnetic field was small ($D < 20$ cm²/sec). The plasma was practically homogeneous along the axis—the density decreased along the system by not more than a factor of two. The temperatures of the electrons and of the ions were identical and close to the ionizer temperature $T_e \approx T_i \sim 0.2$ eV.

PLASMA WAVE INSTABILITY

The linear theory of interaction of a bounded beam with a bounded plasma^[12,13] predicts that under the conditions of our experiment ($v_0 \gg v_{Te}$, $n_0 \gg n_1$, $\omega_{He} \gg \omega_{oe}$) there can take place excitation of Langmuir os-

cillations in the form

$$\varphi(r, \theta, z, t) = \varphi_0 J_m(k_{\perp} r) \exp(i\omega t - im\theta - ik_z z) \quad (1)$$

with a broad frequency spectrum

$$\gamma \sim \frac{k_z}{k} \omega_{0e} \left(\frac{n_1}{n_0} \right)^{1/3}. \quad (2)$$

and an increment

$$\omega \lesssim k_z v_0 \lesssim \omega_{0e} k_z / k \quad (3)$$

The oscillations can have a Cerenkov excitation mechanism ($v_{ph} \sim v_0$) under the condition

$$\frac{\omega}{k_z} \lesssim v_0 < \frac{\omega_{0e}}{k} \left[1 + \frac{3}{2} \left(\frac{n_1}{n_0} \right)^{1/3} \right]. \quad (4)$$

Here v_0 is the velocity of the beam electrons, V_{Te} is the thermal velocity of the plasma electrons, n_1 is the density of the beam electrons, ω_{0e} is the plasma Langmuir frequency, ω_{He} is the electron cyclotron frequency, J_m is a Bessel function of order m , and $k = \sqrt{k_z^2 + k_{\perp}^2}$ is the total wave number. We note that if the beam radius is smaller than the plasma radius R , then the instability increment is smaller than (3) by a factor $\alpha = 1.5(a/R)^{2/3}$ [13]. In our case $\alpha \sim 0.5$.

In the absence of a beam, there are practically no oscillations in the plasma. When a beam passes through a plasma column, excitation of a broad spectrum of HF oscillations is observed in the range 10–1000 MHz. With increasing plasma density, a shift of the oscillation spectrum is observed towards higher frequencies (Fig. 3), and the upper limits of the spectra are located near the electron Langmuir frequencies. No dependence of the frequency or of the amplitude of the oscillations on the magnetic field was observed. These facts are in qualitative agreement with the condition (2).

To explain the spatial structure of the oscillations, we measured the mutual correlation functions and the spatial distribution of the oscillation amplitude. It turned out that the MCF obtained with the probes located in a plane perpendicular to the magnetic field reveal no shifts along the τ axis. The amplitude of the oscillations φ is maximal on the axis and decreases along the radius. The function $\varphi(r)$ can be approximated by a Bessel function $J_0(k_{\perp} r)$. The values of k_{\perp} determined from the Bessel-approximation conditions lie in the range 1–2 cm^{-1} . We can thus state that a standing wave is produced along the radius, corresponding to the azi-

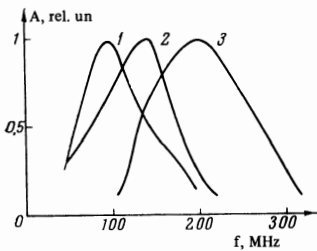


FIG. 3

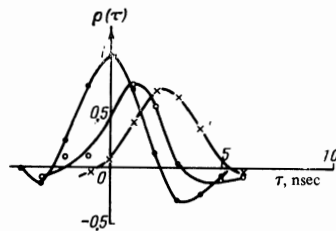


FIG. 4

muthal mode $m = 0$. Figure 4 shows the MCF obtained for different distances Δz between probes. We see that the MCF shifts with increasing Δz , i.e., the oscillations have a longitudinal phase velocity v_{ph} , and accordingly a longitudinal component of the wave vector $k_z = \omega/v_{ph}$. Thus, the excited oscillations have the form

$$\varphi(r, \theta, z, t) = \varphi_0 J_0(k_{\perp} r) \exp(i\omega t - ik_z z).$$

The quantity $v_{ph} = \Delta z/\Delta \tau$, determined from the MCF shift, turns out to be equal to the beam velocity. Thus, for the case of Fig. 4, $v_0 \sim 1 \times 10^9$ cm/sec and $v_{ph} \sim 1 \times 10^9$ cm/sec. The instability is thus excited by the Cerenkov mechanism.

With increasing beam velocity v_0 , the amplitude of the oscillations increases, and then decreases quite sharply. It was observed that for each value of the plasma density there exists a critical value of the beam velocity v_c such that when $v_0 > v_c$ no excitation of the oscillations takes place. Accordingly, when $v_0 = \text{const}$ the excitation occurs at $n_0 > n_c$. It was found that v_c is proportional to $\sqrt{n_0}$ at small beam currents ($n_1 \ll n_0$). The presence of the critical beam velocity and its proportionality to $\sqrt{n_0}$ are in qualitative agreement with the condition (4). It should be noted that relation (4) is well confirmed also qualitatively. For example, for $n_0 \sim 4 \times 10^9$ cm^{-3} the experimental value v_c is 2×10^9 cm/sec and the calculated value is 3×10^9 cm/sec (at $k_{\perp} \sim 1.5$ cm^{-1}).

Thus, the type of the wave, the frequency spectrum, and the mechanism on conditions for the excitation of the oscillations are in good agreement with theory [12, 13]. We can therefore state that excitation of the Langmuir instability is observed in a bounded magnetized plasma.

Measurements were made of the longitudinal distribution of the oscillation amplitude and of the frequency spectra at different distances from the entrance of the beam z . It turned out that in the first 10–20 cm from the beam entrance the amplitude of the oscillations increases exponentially along the beam with an exponential growth coefficient $K_1 \sim 0.1$ cm^{-1} . The oscillation spec-

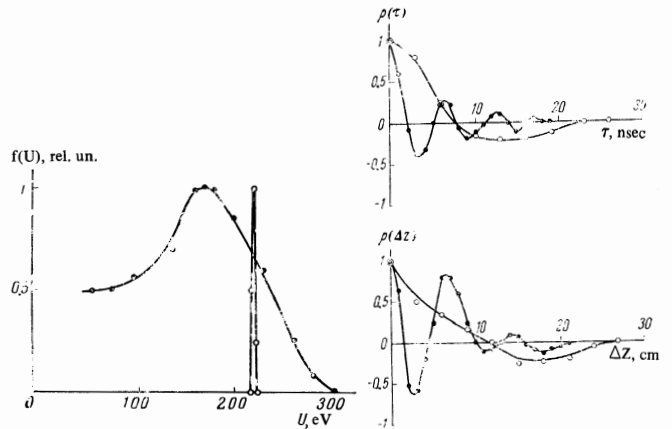


FIG. 5

FIG. 6

FIG. 3. Spectrum of oscillations at different plasma densities: 1— $n_0 \sim 10^8$ cm^{-3} , $U_0 = 90$ eV, $I_0 = 7.5$ mA; 2— $n_0 \sim 4 \times 10^8$ cm^{-3} , $U_0 = 90$ eV, $I_0 = 4.5$ mA; 3— $n_0 \sim 8 \times 10^8$ cm^{-3} , $U_0 = 200$ eV, $I_0 = 3.5$ mA.

FIG. 4. MCF at different distances Δz between probes: ●— $\Delta z = 0$, ○— $\Delta z = 1$ cm, ×— $\Delta z = 2$ cm; $n_0 \sim 3 \times 10^9$ cm^{-3} , $U_0 = 300$ eV, $I_0 = 8$ mA, $n_1 = n_0 \sim 0.02$.

FIG. 5. Beam electron energy distribution functions: ○— $n_0 = 0$, ●— $n_0 \sim 7 \times 10^8$ cm^{-3} ; $U_0 = 220$ eV, $I_0 = 3$ mA, $n_1/n_0 \sim 0.04$.

FIG. 6. ACF (upper figure) and SCF (lower figure) of the potential oscillations in different regimes: ●— $n_0 \sim 2 \times 10^9$ cm^{-3} , $T_e \sim 10$ eV, $U_0 = 240$ eV, $I_0 = 2$ mA, $n_1/n_0 \sim 0.01$; ○— $n_0 \sim 10^8$ cm^{-3} , $T_e \sim 30$ eV, $U_0 = 330$ eV, $I_0 = 19$ mA, $n_1/n_0 \sim 1$.

trum in this section of the plasma column broadens noticeably with increasing distance from the entrance of the beam. At distances larger than 40 cm from the beam entrance, the rate of spatial growth of the amplitude decreases appreciably. The oscillation spectrum in this part of the spectrum is the same at all values of z . Thus, in this part of the plasma column, at distances $\sim 40\text{--}60$ cm from the entrance of the beam, the oscillations are practically stationary and homogeneous. It is precisely in this region that we investigated the turbulent state of the plasma with the aid of correlation measurements.

The spatial growth of the oscillations offers evidence of the convective character of the observed instability. This makes it possible to relate K_1 with the time increment of the growth of the oscillations γ_{meas} :

$$\gamma_{\text{meas}} = K_1 (v_{\text{ph}}^2 v_{\text{gr}})^{1/2} \sim K_1 v_0$$

(Here v_{gr} is the group velocity). It turned out that the values of the calculated and measured increments are in satisfactory agreement. Thus, in the case when $n_1/n_0 \sim 0.04$ we have $(\gamma/\omega)_{\text{calc}} \sim 0.15$ and $(\gamma/\omega)_{\text{meas}} \sim 0.1$.

We measured the energy distribution of the beam electrons. Figure 5 shows the distribution functions $f(U)$ measured by an analyzer located 60 cm away from the entrance of the beam into the plasma. We see that the distribution function of the beam electrons broadens when oscillations are excited. Knowing the distribution function, we can estimate the energy loss of the beam ΔU :

$$\Delta U = U_0 - \bar{U} = U_0 - \int_0^\infty U f(U) dU / \int_0^\infty f(U) dU.$$

It turns out that ΔU is usually 10–15% of the initial beam energy U_0 .

TURBULENT STATE OF THE PLASMA

It was shown earlier that the spectrum of the excited oscillations $\bar{\varphi}(\omega)$ is quite broad and continuous. This indicates that the oscillations of the potential $\varphi(t)$ are irregular and are random in time. We can expect these oscillations to be likewise irregular in space. It was observed in the experiment that at all amplitudes and at all radii of the plasma column (at $z = \text{const}$) the oscillations are correlated and the spatial irregularity takes place only with respect to the coordinate z . The qualitative characteristics of the degree of irregularity of the oscillations are the time and length of the correlation, determined respectively from the ACF and the SCF. Figure 6 shows the ACF $\rho(\tau)$ and the SCF $\rho(\Delta z)$ of the Langmuir oscillations, measured in two regimes having different beam powers and plasma densities (and naturally different average frequencies). In one regime, the parameter n_1/n_0 amounted to 0.01, and in the other $n_1/n_0 \sim 1$. We see that the correlation time and length decrease with increasing n_1/n_0 , reaching one period of the average frequency and one average wavelength at $n_1/n_0 \sim 1$. Thus, the oscillations become strongly randomized in time and in space with increasing n_1/n_0 .

A characteristic of the turbulence is, as is well known, the spectral density of the power (energy) $\varphi_{k\omega}^2 (E_{k\omega}^2)$. Since in our case the turbulence was practically homogeneous, we determined in the experiment

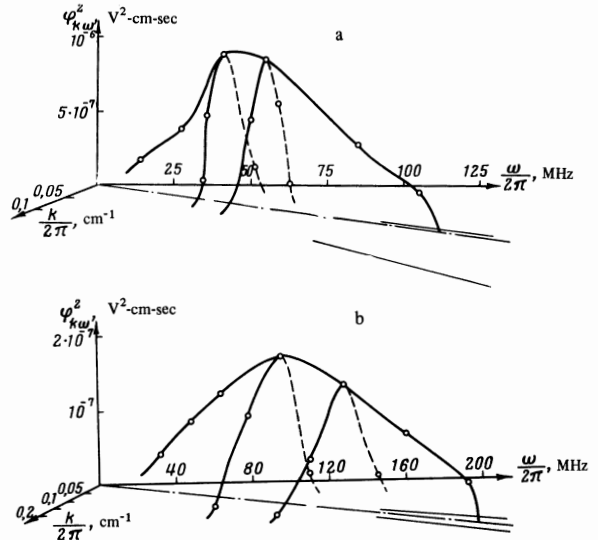


FIG. 7. $\varphi^2_{k\omega}$ spectra in different regimes: a— $n_0 \sim 7 \times 10^8 \text{ cm}^{-3}$, $U_0 = 220 \text{ eV}$, $I_0 = 3 \text{ mA}$, $n_1/n_0 \sim 0.04$, $T_e \sim 8 \text{ eV}$; $\bar{\varphi} \sim 11 \text{ V}$, $E^2/8\pi n_0 T_e \sim 2 \times 10^3$; b— $n_0 \sim 2 \times 10^8 \text{ cm}^{-3}$, $U_0 = 240 \text{ eV}$, $I_0 = 6 \text{ mA}$, $n_1/n_0 \sim 0.3$; $T_e \sim 20 \text{ eV}$, $\bar{\varphi} \sim 11 \text{ V}$, $E^2/8\pi n_0 T_e \sim 10^2$.

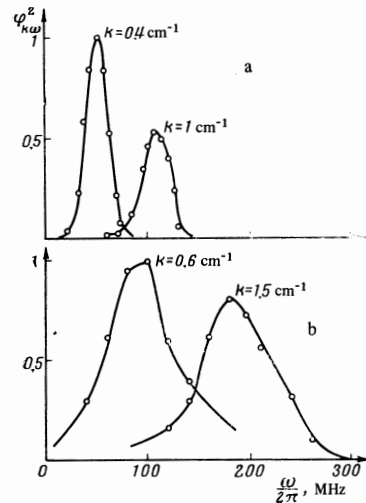


FIG. 8. Packets of $\varphi^2_{k\omega}$ for the same regimes as in Fig. 7.

the spectrum $\varphi^2_{k_z\omega}$ (for convenience, we shall henceforth use k for k_z). To this end we measured the space-time correlation function STCF $\rho(\Delta z, \tau)$. The measurements were performed in several regimes having different values of n_1/n_0 .

Figure 7 shows the $\varphi^2_{k\omega}$ spectra for the cases $n_1/n_0 = 0.04$ and $n_1/n_0 = 0.3$. The thin lines in the (k, ω) plane delineate the boundaries of the region where $\partial f/\partial v > 0$, f —the distribution function of the beam electrons, measured simultaneously with $\varphi^2_{k\omega}$. We see that the maximum amplitudes of the spectrum $\varphi^2_{k\omega}$ lie precisely in this region, indicating that the oscillations build up by the Cerenkov mechanism (the mechanism of inverse Landau damping). We call attention to the fact that the projection of the maximum amplitude of the spectrum on the (k, ω) plane is a straight line $\omega_k/k = \text{const}$, i.e., it is single-valued (one value of k corresponds to one value of ω), as follows from the linear theory for the

case when k_{\perp} is approximately the same for all the harmonics. On this basis we can represent the $\varphi_{k\omega}^2$ spectrum in the form of a set of harmonics with different values of k .

Figure 8 shows the spectrum of $\varphi_{k\omega}^2(\omega)$ for two k -packets in each regime. We see that each packet has a finite width $\Delta\omega_k$, which increases with increasing n_1/n_0 . Thus, at $n_1/n_0 = 0.04$, we have $\Delta\omega_k/\omega_k = 0.25$, and at $n_1/n_0 = 0.3$ it increases to 0.45. The presence of a finite width of the packets indicates that each k -th harmonic of the oscillations, unlike the concepts of the quasilinear theory, is not monochromatic, i.e., it is irregular, and has a finite correlation time $\tau_k \sim 1/\Delta\omega_k$. In both regimes, the value of $\Delta\omega_k$ is close to the calculated value of the linear increment γ_k , since the values of γ_k/ω_k are respectively 0.15 and 0.35. It thus turns out that $\tau_k \sim 1/\gamma_k$. The possible causes of such an irregularity will be discussed below, after reporting the results on the heating of the plasma electrons.

HEATING OF ELECTRONS

As already mentioned, in the absence of a beam the longitudinal electron temperature, measured with the aid of the analyzers, amounts to ~ 0.2 eV. The "limiting" electron energy ϵ amounts in this case to ~ 0.7 eV. When the beam passes through a plasma column, the appearance of electrons accelerated in a longitudinal direction is observed simultaneously with excitation of the high frequency oscillations. Their presence is revealed by the increase of the "limiting" energy, which in some cases exceeds 100 eV. Accelerated electrons are observed at all radii within the confines of the plasma column, and electrons accelerated in both the beam direction and in the opposite direction are registered. On the basis of this, the electrons are of plasma origin.

The measurements of the plasma electron deceleration curves have shown that as a rule the electron velocity distribution function $f(v_z)$ is Maxwellian and can be characterized by a longitudinal temperature T (henceforth denoted as T_e). This is seen in Fig. 9, which shows several $\log I(V)$ curves plotted with an energy analyzer at different values of the beam energy. We note that when $U_0 > U_c$, when the excitation of the high frequency oscillations stops, the temperature T_e becomes equal to 0.2 eV. On the basis of these factors, it can be stated that experiment reveals heating of the plasma electrons in the fields of the high frequency oscillations. The value of T_e is practically the same at all radii of the plasma column and does not depend on z . The maxi-

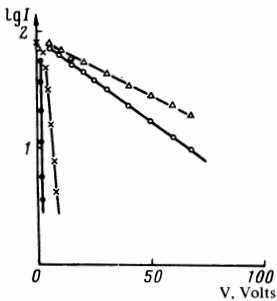


FIG. 9. Current-voltage characteristics of the analyzer in different regimes (the analyzer is at a radius exceeding the beam radius): \bullet — $n_0 \sim 6 \times 10^9 \text{ cm}^{-3}$, $U_0 = 0$, $I_0 = 0$, $T_e \sim 0.2$ eV, \times — $n_0 \sim 10^9 \text{ cm}^{-3}$, $U_0 = 45$ eV, $I_0 = 5$ mA, $T_e \sim 2$ eV; \circ — $n_0 \sim 2 \times 10^8 \text{ cm}^{-3}$, $U_0 = 100$ eV, $I_0 = 7$ mA, $T_e \sim 30$ eV; Δ — $n_0 \sim 10^8 \text{ cm}^{-3}$, $U_0 = 180$ eV, $I_0 = 8$ mA, $T_e \sim 50$ eV.

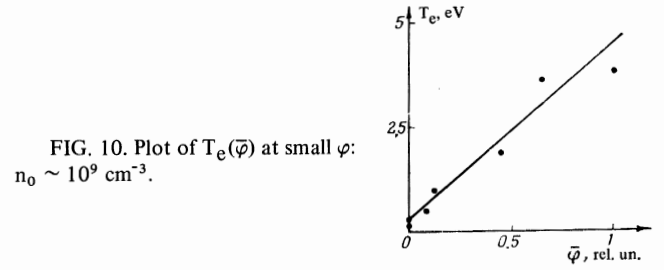


FIG. 10. Plot of $T_e(\bar{\varphi})$ at small φ : $n_0 \sim 10^9 \text{ cm}^{-3}$.

mum values of T_e , observed in the experiment, reached 50 eV.

We estimated what fraction of the energy lost by the beam in the plasma goes to electron heating. To this end, the flux of the energy lost by the beam $J = I_0 \Delta U$ was compared with the energy taken out of the beam by the heated electrons (J_T) and by the oscillations (J_E). Since the plasma was collisionless, it was reasonable to assume that the main mechanism of electron loss is escape from the ends along the magnetic field. In this case $J_T = (1/4)n_0 v_T T_e S$ if $T_{\perp} \ll T_{\parallel}$ (this assumption is reasonable, since $\omega \ll \omega_{He}$ and $T_{\perp 0} \sim 0.2$ eV). An estimate shows that the diffusion flux across the field is negligibly small compared with J_T . The flux J_E can be estimated by taking into account the fact that the group velocity of the oscillations is close to v_{ph} : $J_E = (\bar{E}^2/8\pi)v_{Th}S$. Since $\bar{E}^2/8\pi n_0 T_e$ is small (usually $\bar{E}^2/8\pi n_0 T_e = (k_z^2 + k_{\perp}^2)\bar{\varphi}^2/8\pi n_0 T_e \lesssim 10^{-2}$), J_E amounts to a small fraction of J_T (estimated at 10–20%).

A comparison of J_T and J for several regimes shows that practically the entire energy lost by the beam goes to heating of the plasma electrons:

$J, W:$	0.1	0.3	0.5	0.5
$J_T, W:$	0.1	0.3	0.4	0.5

As already noted, the amplitude of the oscillations depends on the beam energy U_0 . At small electron-beam powers, when the amplitude of the oscillations in the plasma is relatively small, the plasma density and the frequency spectrum of the excited oscillations depend little on U_0 , so that by varying U_0 it is possible to obtain the dependence of T_e on the amplitude $\bar{\varphi}$ with the remaining parameters constant. It turns out that in this case $T_e \propto \bar{\varphi}$ —see Fig. 10. With increasing beam power, when the plasma density and the oscillation frequency spectrum begin to change, this dependence becomes more complicated. As shown by correlation measurements, an increase of T_e occurs also when the time and the correlation length of the oscillations decrease. Large values of T_e are reached in the case of strong turbulence of the oscillations.

Let us consider the possible mechanism of electron heating. Since the average phase velocity of the oscillations greatly exceeds the thermal velocity of the plasma electrons ($v_{ph} \sim v_0 \gg v_{Te}$), the resonant interaction between the oscillations and the plasma electrons is excluded; the observed electron heating is obviously due to a nonresonant mechanism. The interaction of the oscillations with the nonresonant electrons, within the framework of the quasilinear theory, is described by the formulas^[14]

$$\frac{dT_e}{dt} = \frac{e^2}{2m} \sum_k \frac{\gamma_k E_k^2}{\omega_k^2 + \gamma_k^2} \approx \frac{e^2}{2m} \sum_k \frac{\gamma_k E_k^2}{\omega_k^2}, \quad \gamma_k^2 \ll \omega_k^2, \quad (5)$$

where the longitudinal component of the electric field of the k -th harmonic E_k and γ_k are connected by the equation

$$\frac{d}{dt} E_k^2 = 2\gamma E_k^2 \quad (6)$$

Substituting (6) in (5) and integrating with respect to time, we get

$$T_e(t) = \frac{e^2}{2m} \sum_k \frac{E_k^2(t)}{2\omega_k^2} + T(0). \quad (7)$$

It is seen from (7) that quasilinear nonresonant heating is reversible—the electron temperature T_e is proportional to the value of E^2 at a given instant of time, so that when the electric field is turned off T_e decreases to the initial value $T_e(0)$. We call attention to the fact that for reversible heating the following relation is satisfied^[14]

$$E^2 / 8\pi n_0 T_e \sim 1. \quad (8)$$

In the experiment, the value of $E^2 / 8\pi n_0 T_e$ amounts to $\lesssim 10^{-3}$ at the entrance of the beam into the plasma and $\lesssim 10^{-2}$ in the region of the ionizer. Thus, T_e is larger by two or three orders of magnitude than it should be in accord with (8), i.e., the observed heating is not reversible and consequently cannot be described within the framework of the quasilinear theory.

Such ‘‘classical’’ nonlinear processes of decays or stimulating scattering of waves by plasma electrons cannot ensure in our case either the observed $T_e(E)$ dependence or the observed value of T_e . Indeed, the decays are in general forbidden processes by virtue of the form of the dispersion curve of the oscillations, and the estimate of the heating effect due to the induced scattering, based on the formulas of^[15], yields a value of T_e which is smaller by four or five orders of magnitude than the observed value, and yields a dependence $T_e \propto E^4$ (with allowance for the condition for the balance of the energy fluxes (see below) we get $T_e \propto E^{8/3}$), which differs from the experimental one ($T_e \propto \bar{\varphi} \propto \bar{E}$).

On the basis of the qualitative dependences of T_e on $\bar{\varphi}$ and on the correlation time, it was proposed that the heating has a stochastic nature and the experimental results were compared with the semiphenomenological theory given in^[16-18], where the interaction of plasma electrons with a stochastic field was considered. Assuming that the spectrum of the oscillations $E_{k\omega}^2$ can be represented in the form of a sum of k -packets

$$E_{k\omega}^2 = \sum_k \frac{E_k^2 \tau_k}{1 + (\omega - \omega_k)^2 \tau_k^2}, \quad (9)$$

and also assuming $\omega_k/k \gg v_{Te}$, Bass, Faïnberg, and Shapiro^[16] obtained the following connection between the longitudinal electron temperature and the characteristics of the oscillations:

$$\frac{dT_e}{dt} = \frac{e^2}{2m} \sum_k \frac{E_k^2 \tau_k}{1 + \omega_k^2 \tau_k^2}. \quad (10)$$

Since it turned out that the experimentally measured spectra $E_{k\omega}^2 = k^2 \varphi_{k\omega}^2$ are satisfactorily described by formula (9), all the quantities in (10) can be determined experimentally:

$$E_k^2 = k^2 \int \varphi_{k\omega}^2 d\omega, \quad \tau_k \sim \frac{1}{\Delta\omega_k}.$$

To compare formula (10) with experiment, it is necessary to take into account the fact that in the sta-

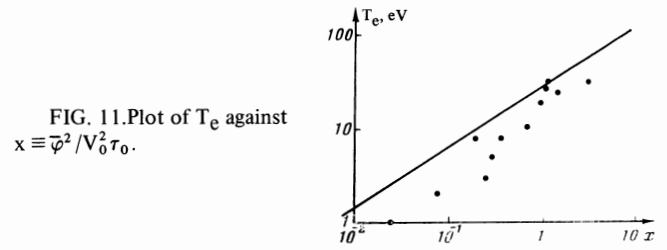


FIG. 11. Plot of T_e against $x \equiv \bar{\varphi}^2 / v_0^2 \tau_0$.

tionary state ($dT_e/dt = 0$) the flux of energy obtained by the electrons from the oscillations

$$n_0 L S \frac{e^2}{2m} \sum_k \frac{E_k^2 \tau_k}{1 + \omega_k^2 \tau_k^2}$$

is equal to the flux of energy to the ends J_T . The net result is

$$T_e = \left(\sqrt{\frac{\pi}{2m}} e^2 L \sum_k \frac{E_k^2 \tau_k}{1 + \omega_k^2 \tau_k^2} \right)^{3/2}. \quad (11)$$

Here L is the length of the plasma column.

Comparison of the temperature calculated in accordance with (11) with that measured experimentally was carried out in two regimes. The results are:

T_e^{exp} , eV	8,5	20
T_e^{calc} , eV	17	40

Recognizing the approximate character of the formula and the measurement errors, we can assume that the experimental values of T_e are in satisfactory agreement with the calculated ones.

Introducing the assumption that $\tau_k \approx \tau_0$ (τ_0 is the correlation time determined from the ACF), we can greatly simplify formula (11). Indeed, since $\omega_k/k \approx v_0$, $E_k^2 = k^2 \tau_k^2$, and $\omega_k^2 \tau_k^2 \gg 1$ for the measured spectra, we get

$$\sum_k \frac{E_k^2 \tau_k}{1 + \omega_k^2 \tau_k^2} \approx \sum_k \frac{\varphi_k^2 k^2}{\tau_0 \omega_k^2} \approx \frac{\bar{\varphi}^2}{v_0^2 \tau_0}. \quad (12)$$

Accordingly we now get in place of (11)

$$T_e \approx \left(\sqrt{\frac{\pi}{2m}} e^2 L \frac{\bar{\varphi}^2}{v_0^2 \tau_0} \right)^{3/2}. \quad (13)$$

Figure 11 shows the dependence of T_e on the parameter $x \equiv \bar{\varphi}^2 / v_0^2 \tau_0$. The straight line corresponds to the calculated and the points to the experimental values of T_e . We see that both the $T_e(x)$ dependence and the absolute values of T_e are in satisfactory agreement with calculation. We note that the dependence of the electron temperature on the amplitude $T_e \propto \bar{\varphi}$ (Fig. 10) is close also to the calculated $T_e \propto \bar{\varphi}^{4/3}$.

Thus, the observed heating is well described by the phenomenological theory of stochastic heating. Attention must be called, however, to the following circumstances: formula (10), which describes the heating of the nonresonant particles, was obtained in the quasilinear approximation for an external electric field. In the case of a self-consistent field, within the framework of the quasilinear approximation, its spectrum $E_{k\omega}^2$ cannot be obtained in the form (9), proposed in^[16]. Indeed, a field satisfying (9) is stationary and its spectrum consists of k -packets of finite half-width $\Delta\omega_k \sim 1/\tau_k$. At the same time, in the quasilinear theory the spectrum of the stationary field consists of a set of packets with $\Delta\omega_k \sim 0$,

$E_{k\omega}^2 = E_k^2 \delta(\omega - \omega_k)$ (the weak-turbulence approximation). Therefore a field of the form (9) can be obtained only when account is taken of the nonlinear interaction of the oscillations with the plasma. It might seem that in this case the behavior of the nonresonant electrons should be described not by the "quasilinear" formula (10), but by formulas that take nonlinear effects into account. However, experiment shows that although the oscillation spectrum has a form close to (9), the observed heating is described nonetheless by the quasilinear formula. This fact indicates that there exist nonlinear interactions that determine the spectrum of the field, such in which no account is taken of the main part of the plasma electrons.

Such an effect may be the capture of the beam electrons by a wave of finite amplitude $\bar{\varphi}$ ^[19,20]. Indeed, since γ/ω is not very small, the amplitude increases quite rapidly, so that the number of captured electrons (the velocity interval $\omega_k/k \pm \sqrt{2e\bar{\varphi}/m}$) increases and is not small. As a result, the interaction of the captured electrons with the wave can lead to strong changes of the field of the wave. For nonresonant plasma electrons, this field plays the role of a randomly varying external field, the interaction with which leads to their heating. The mechanism causing wave attenuation is the transfer of energy to the plasma electrons.

The changes of the wave field as a result of the interaction between the wave and the captured electrons are equivalent to broadening of the spectrum $\varphi_{k\omega}^2$ relative to the frequency of the k-harmonics. Obviously, the stationary state is attained when the effective damping decrement becomes equal to the linear increment γ_k . The width $\Delta\omega_k$ of the spectrum of the k-th harmonic should in this case be approximately equal to γ_k , as is indeed observed experimentally.

We note that the number of oscillations that the electron has time to execute in the "potential well" of the wave during the time of "flight" of the wave through the column is small:

$$m \sim \frac{L}{v_{ph}} / \frac{\lambda}{\sqrt{e\bar{\varphi}/m}} \sim 1-2.$$

As a result, the mechanism of phase mixing^[20] may not operate, and this can cause the absence of a broad plateau on the distribution function of the beam.

When the plasma electron temperature increases, an important role may be assumed by capture of electrons from the "tail" of the distribution function by the wave. Such an effect was observed in the numerical experiments of Dawson and Shanny^[21], devoted to an investigation of the damping of a wave of finite amplitude ($v_{ph} > v_{Te}$) in a plasma with a Maxwellian distribution. In the case $\sqrt{2e\bar{\varphi}/m} < v_{ph}$ it was found that capture from the "tail" of the distribution function leads to an appreciable increase of the damping decrement when the ratio $v_T/v_{ph} \gtrsim 0.3$. This value of v_T/v_{ph} is reached in our experiment at $T_e \sim 20$ eV.

In the numerical experiments of Bers and Davis^[22], devoted to the interaction of a beam with a plasma, capture of a small fraction of the plasma electrons was also observed. With increasing number of captured electrons, an irregular change of the field of the oscillations was observed and appreciable heating of all the plasma electrons.

In conclusion, the authors consider it their pleasant duty to thank Ya. B. Faïnberg, V. D. Shapiro, D. D. Ryutov, and V. N. Tsytovich for useful discussions, Yu. I. Ėidel'man for help with the experiments, and V. N. Kheifets for performing the calculations.

¹ Ya. B. Faïnberg, in: Fizika plazmy i problemy upravlyaemogo termoyadernogo sinteza (Plasma Physics and the Problem of Controlled Thermonuclear Fusion), v. 2, Ukr. Acad. Sci, 1963, p. 88; Usp. Fiz. Nauk 93, 617 (1967) [Sov. Phys.-Uspekhi 10, 750 (1968)].

² A. K. Berezin, G. P. Berezina, L. I. Bolotin, and Ya. B. Faïnberg, Atomnaya énergiya 14, 249 (1963).

³ R. A. Demirkhanov, A. V. Gevorkov, A. F. Popov, G. L. Kharasanov, Proc. Conf. Plasma Physics and Contr. Nuclear Fusion Research, v. 2, IAEA, Vienna, 1966, p. 801. L. D. Smullin and W. D. Getty, *ibid.* p. 815.

⁴ V. M. Nezhlin and A. M. Solntsev, Zh. Eksp. Teor. Fiz. 48, 1237 (1965) [Sov. Phys.-JETP 21, 826 (1965)].

⁵ I. Alexeff and R. V. Neidigh, Phys. Rev. 136, 689 (1964); R. V. Neidigh, I. Alexeff, and G. E. Guest et al., Proc. Conf. Plasma Physics and Contr. Nuclear Fusion Research, 2 IAEA Vienna, 1969, p. 693.

⁶ E. A. Kornilov, Ya. B. Faïnberg, and O. F. Kovpik, ZhETF Pis. Red. 4, 147 (1966) [JETP Lett. 4, 101 (1966)].

⁷ Yu. G. Yaremenko, V. M. Deev, R. L. Slabovik, and I. F. Kharchenko, Atomnaya énergiya 25, 213 (1967).

⁸ I. Alexeff, G. E. Guest, D. C. Montgomery, R. V. Neidigh, and D. J. Rose, Phys. Rev. Lett. 21, 344 (1968).

⁹ Yu. I. Kagan and V. I. Perel', Usp. Fiz. Nauk 81, 409 (1963) [Sov. Phys.-Uspekhi 6, 769 (1964)].

¹⁰ I. S. Fishman and N. P. Mukhortov, PTÉ No. 5, 110 (1969).

¹¹ I. S. Fishman, PTÉ, 1970, in press.

¹² M. F. Gorbatenko, Zh. Tekh. Fiz. 33, 1070 (1963) [Sov. Phys.-Tech. Phys. 8, 798 (1964)].

¹³ R. J. Briggs, Electron-Stream Interaction with Plasma, M.I.T. Press, Cambridge (1964).

¹⁴ V. D. Shapiro, Zh. Eksp. Teor. Fiz. 44, 613 (1963) [Sov. Phys.-JETP 17, 416 (1963)].

¹⁵ V. G. Makhan'kov and V. N. Tsytovich, Stochastic Heating of Plasma Particles, JINR Preprint, Dubna, 1968.

¹⁶ F. G. Bass, Ya. B. Faïnberg, and V. D. Shapiro, Zh. Eksp. Teor. Fiz. 49, 329 (1965) [Sov. Phys.-JETP 22, 230 (1966)].

¹⁷ P. A. Sturrock, Phys. Rev. 141, 186 (1966).

¹⁸ S. Puri, Phys. Fluids 9, 2043 (1966).

¹⁹ T. H. Dupree, Phys. Fluids 9, 1773 (1966).

²⁰ B. B. Kadomtsev, Usp. Fiz. Nauk 95, 111 (1968) [Sov. Phys.-Uspekhi 11, 328 (1968)].

²¹ J. M. Dawson and R. Shanny, Phys. Fluids 11, 1506 (1968).

²² A. Bers and J. A. Davis, Nonlinear Aspects of the Beam-Plasma Interaction, Review Paper delivered at the Third European Conference on Plasma Physics and Controlled Fusion, Utrecht, 1969.